5-16-2012

Fragmentation of explosively metastable glass [post-print]

Mark P. Silverman
Trinity College, mark.silverman@trincoll.edu

Wayne Strange
Trinity College

J. Bower

L. Ikejimba

IOP PUBLISHING
Phys. Scr. **85** (2012) 065403 (9pp)

PHYSICA SCRIPTA
doi:10.1088/0031-8949/85/06/065403

Fragmentation of Explosively Metastable Glass

M. P. Silverman[(a)], W. Strange, J. Bower, L. Ikejimba[(b)]
Department of Physics, Trinity College, Hartford CT 06120 USA

PACS: 46.50.+a (fracture mechanics, fatigue and cracks);
62.20.mm- (fracture);
62.50.Ef (shock wave effects in solids and liquids)
64.60.ai (fractal and multifractal systems)

Abstract

An unusual form of glass with bulbous head and thin tail, known as Rupert's drops, can withstand high impact or pressure applied to the head, but explodes instantly into small particles when the tail is broken. The mechanism is not well understood. To examine this, we performed macro- and microstatistical analyses of a sample of 500 g of fragments of exploded Rupert's drops to determine the mass and particle distributions and associated fractal dimensions. To our knowledge, this is the first such statistical study of the fragmentation of a metastable material with large internal energy. The resulting fractal dimension $D = 1.06 \pm 0.09$, derived from the scaling region of the mass and particle distribution functions approximated by power laws, differs from fractal dimensions (usually ≥ 2) previously reported for many brittle materials. The observed distribution functions place constraints on proposed mechanisms for the explosive disintegration of the drops and presumably other physical systems characterized by high compressive stress at the surface and tensile stress within the core.

[(a)] Contact: **mark.silverman@trincoll.edu**
[(b)] Current address: Graduate Program in Medical Physics, Duke University, Durham NC 27705

PHYSICA SCRIPTA
doi:10.1088/0031-8949/85/06/065403

1. Introduction

Fragmentation plays a critical role in many areas of physics among which are geophysics (e.g. fracture of rocks) [1], planetary science (e.g. meteoritic impact) [2], astrophysics and cosmology (e.g. interstellar grain, asteroid, and galaxy formation; evolution of the universe) [3,4]; nuclear physics (e.g. spallation processes) [5], statistical physics (e.g. critical phenomena) [6], and materials science (e.g. energetics of materials) [7] as well as to fields of engineering (e.g. chemical combustion) [8] and industry (e.g. mining) [9]. Although a wide range of mechanisms comes into play, many fragmentation processes, particularly those involving rapid events such as explosions and collisions, appear to exhibit universality [10,11] leading to power-law behavior over a limited range of fragment sizes or masses. To our knowledge, the statistical investigation of the fragmentation of materials hitherto reported all involved passive materials subjected to external forces. In this paper we report the statistical examination of fragments derived from a material in an explosive metastable state of very high surface compression and core tension.

The material referred to as Rupert's drops is an unusual form of tempered (i.e. thermally toughened) glass known in Europe for over 300 years and quite possibly since the time of ancient Rome [12]. It is made by letting molten glass, heated by torch or drawn from an oven, fall freely under gravity into a receptacle of cold water. Implemented appropriately, the glass does not shatter, but forms a tadpole-shaped droplet with bulbous head and long thin tail. Since the exterior rapidly cools before the interior, the outer layer of a Rupert's drop is highly compressed while the core is subject to large tension. Examined between crossed polarizers (Figure 1), the drops display a pronounced stress-induced birefringence.

As a consequence of these large compressive and tensile stresses, the head of the glass drop can be struck with a hammer or squeezed with pliers without damage—yet the drop explosively disintegrates into small particles (Figure 2) if the thin tail is snapped off. Ordinary tempered glass, such as used for windows in motor cars, does not explode upon rupture, but merely breaks into small cubical fragments. This surprising transformation has long served as a source of amusement [13], yet to our knowledge relatively few scientific studies have been made of it. In particular, the precise mechanism of the explosion remains to be explained satisfactorily. Previous high-speed photographic studies suggested that disintegration of Rupert's drops proceeded by crack bifurcation [14, 15].

A complementary way of elucidating the mechanism of fragmentation is by statistical analysis of the fragments. Studies of fragments of diverse materials (rocks, coal, sand, clay, glacial till, interstellar grains, and more) produced by a wide array of disintegrative processes (abrasion, ballistic impact, chemical explosion, nuclear explosion, and more) have been found to be characterized to good approximation by a particle distribution function [16]

$$N(s) \equiv \int_{s}^{s_{\max}} n(s')\,ds' = C_N\left(s^{-D} - s_{\max}^{-D}\right) \approx C_N s^{-D} \tag{1}$$

where $N(s)$ is the number of particles of size (e.g. diameter) $\geq s$,

$$n(s) = -dN(s)/ds = C_N D s^{-D-1} \tag{2}$$

is the particle density function, $s_{\max}$ is the largest size in the sample, and C_N and D are constants. Over a range of sizes $s < s_{\max}$ for which the term $s_{\max}^{-D}$ in Eq. (1) can be disregarded, $N(s)$ follows a power law with D defined by Mandelbrot as the fractal dimension [17].

The fractal dimension, which can be defined operationally in other ways equivalent to Eq. (1) for self-similar objects, is a statistical measure of how much space these objects occupy under a transformation of scale. We use the noncommittal term "space" to refer to length, area, or volume, depending on the topological dimension d (1, 2, or 3) of the space in which the objects are embedded. Values of D reported for fragments of passive materials like those cited above fell in the range ~1.5-3.5, with the preponderance of values in the vicinity of ~2.5. In this paper we

report the value $D_{\mathrm{RD}} = 1.06 \pm 0.09$ for fragments obtained from approximately 50 exploded lead-crystal glass Rupert's drops of transverse head diameter ~1.0-1.5 cm and total drop length ~7-12 cm to produce an initial aggregate mass of 514.49 g of fragments.

2. Analytical Procedures

In the statistical analysis of a sample of fragments containing many small particles, it is usually not practicable to determine $N(s)$ by direct counting. Instead, one determines the mass density function $m(s)$—i.e. mass of particles within the range $(s, s+ds)$—and corresponding cumulative distribution

$$M(s) \equiv \int_{s_{\mathrm{min}}}^{s} m(s')ds' = C_M \int_{s_{\mathrm{min}}}^{s} s^d n(s')ds' \tag{3}$$

yielding the mass of particles of size $\leq s$, with s_{min} the smallest size in the sample. A mass-based approach is considered more sensitive to deviations from linearity [18]. For a material with constant mass per volume[1] at fixed temperature, the mass and particle density functions of self-similar particles are related by $m(s) \propto s^d n(s)$ with $d = 3$ for glass fragments. The proportionality constant C_M depends on the geometry of the particles. Assuming the power law expression in Eq. (1), one can show that

$$M(s) = M_0 \left(s^{d-D} - s_{\mathrm{min}}^{d-D} \right) \Big/ \left(s_{\mathrm{max}}^{d-D} - s_{\mathrm{min}}^{d-D} \right) \approx M_0 \left(s / s_{\mathrm{max}} \right)^{d-D} \tag{4}$$

where M_0 is the total sample mass, and the approximate equality follows when one can neglect s_{min}. From the preceding discussion, there then follow in principle four ways to deduce the fractal dimension from the slope of double-log plots of particle and mass distributions as a function of size:

$$\begin{aligned} &(\mathrm{a})\ d\log N(s)/d\log s = -D_N && (\mathrm{c})\ d\log M(s)/d\log s = d - D_M \\ &(\mathrm{b})\ d\log n(s)/d\log s = -D_n - 1 && (\mathrm{d})\ d\log m(s)/d\log s = d - D_m - 1 \end{aligned} \tag{5}$$

where subscripts on *D* designate the parent function. The resulting slopes are independent of the logarithm base or units of size and mass.

We refer to these methods as macrostatistical, since they involve measurements on a sample of many particles at a time. In an actual experiment, a sample of fragments is partitioned by size into discrete classes (bins) by means of calibrated sieves. To determine the fractal dimension of the Rupert's drops fragments, we have used relations (5a) and (5c), where $N(s)$ in expression (5a) was determined from the mass density function through the inverse relation $n(s) \propto s^{-d} m(s)$. Mass- and count-based estimates of D_N have been shown to be nearly the same for scale-invariant aggregates [19]. Because fragment length varies continuously, the use of a cumulative distribution rather than density function leads to more consistent values of fractal dimension [20].

Another method of obtaining fractal dimension, which we refer to as microstatistical, is to relate the perimeter to the area of individual fragments in a representative statistical sample. According to Mandelbrot [21], the length and area of a fractal geometric object satisfy the relation $P \propto A^{D/2}$. Thus, the slope of a double-log plot of perimeter against area for a random sample of self-similar particles yields a geometry-based fractal dimension

$$D_g = 2\, d\log P / d\log A\,. \tag{6}$$

[1] We refrain from using the familiar term "density" for the macroscopic mass per volume to avoid confusion with the particle and mass statistical densities.

Mandelbrot's theoretical construction for estimating *D* entailed measuring the size of a fixed object with a variable scale ("box counting")—i.e. taking a limit of the variation in size as the scale is reduced. In the practical analysis of fragments, however, one does the equivalent by measuring the size of a variable object (the different fragments) with a fixed scale [16]. Since the fractal dimension is completely determined by the slope of the line of regression in a scatter plot, all that is necessary is that samples be chosen that span the range of sizes within which the preponderance of fragments fall.

An assumption, either explicitly stated or implicit in the use of relations 5a-d, underlying previous determinations of the fractal dimensions of fragments of passive materials is that fragment morphology is independent of size—i.e. that sampled particles are self-similar for purposes of analysis. The assumption is readily verified for particles of the same smooth geometric shape (e.g. spherical glass beads). However, for processes like explosive fragmentation that give rise to irregularly shaped particles, the assumption of self-similarity is not easily confirmed or refuted beforehand by direct visual appearance. Supportive evidence may be adduced afterward if different empirical procedures for determining fractal dimension all yield the same numerical value. Our examination of randomly selected Rupert's glass fragments under a stereomicroscope gave no reason to suggest that fragments in the total population may have constituted samples drawn from physically distinct subpopulations described by different mass or particle distributions. We have therefore made the assumption of self-similarity in this analysis so that we could compare the resulting fractal dimensions of Rupert's drops with fractal dimensions obtained by similar methods for previously investigated passive materials.. We return to this point, however, in our concluding remarks.

3. Experimental Results

A sample of ~500 g of lead-crystal Rupert's drops fragments was partitioned into ten classes by sieving with a set of woven wire or cloth mesh sieves of standard mesh sizes (in microns) of 4000, 2000, 1000, 707, 500, 354, 250, 177, 125, and 88. The observed mass density function shown in Figures 3a,b is reasonably well accommodated by a log hyperbolic density [22]

$$m(s) = Ae^{-a\sqrt{\left(\frac{\ln(s/s_0)}{\delta}+1\right)}+b\left(\frac{\ln(s/s_0)}{\delta}\right)}, \qquad (7)$$

the parameters of which are interpreted as follows: $\mu \equiv \ln s_0$ is a location parameter (determines peak), δ is a scale parameter (determines width), and *a* and *b* together determine the left and right asymptotic slopes $\varphi_{\pm} = \pm(a \pm b)$ of the hyperbolic function of size *s* in the exponent. The amplitude *A* is a normalization constant expressible as a modified Bessel function of the second kind. As limiting cases, the log hyperbolic density reduces to a log normal density for large δ and to a log skew-Laplace density for vanishing δ.

The dashed curves shown in Figures 3a,b were fit visually rather than by a statistical fitting procedure (since no frequency-based measures of goodness-of-fit are available for fitting models to an empirical mass size distribution [23]) and serve primarily for comparative purposes. The double-log plot in Figure 3b shows the approximate hyperbolic form of the functional dependence on size in the exponent of Eq. (7) suggesting that the cumulative mass distribution $M(s)$ should approximate power law behavior over the range of sizes comprising the φ_+ asymptote.

1. *Determination of D from* $M(s)$

Following standard procedure, $\log M(s_i)\ (i = 1 \ldots 10)$ was plotted against the log of the mean bin size $(s_i + s_{i-1})/2$ (with $s_0 \equiv 0$) as shown in Figure 4, and a least-squares line of regression was fit to all but the final point (corresponding to $s_{\max}$). From Eq. (5c) with $d = 3$ we

obtained $D_M = 1.17 \pm 0.12$. The estimated uncertainty of D_M (and D_N below) takes account of uncertainties in both ordinate and abscissa due to finite bin widths [24, 25].

2. *Determination of D from* $N(s)$

Using the relation $n(s) \propto s^{-d} m(s)$ of Eq. (3), with $d = 3$, we constructed the distribution

$$N(s_i) = N_0 \left(1 - \sum_{k=1}^{i} s_k^{-d} m(s_k) \right) \tag{8}$$

where N_0 is a normalizing constant, shown in Figure 5a. From the corresponding double-log plot of Figure 5b, it is seen that $N(s)$ followed a power law in s to good approximation except for two points at the largest size bins, which were excluded from the regression analysis. The slope of the line of regression led to $D_N = 1.01 \pm 0.08$.

3. D*etermination of D from* $P \propto A^{D/2}$

Using a stereomicroscope with digital camera and particle counting software, we determined the length L, width W, mean size $(L+W)/2$, perimeter P, and area A of each fragment in a randomly chosen sample of 151 fragments. The fractal relation is not particularly sensitive to which linear measure of size is used. The histogram in Figure 6a presents a frequency distribution of particles classified according to mean size. The randomness of fragment selection is supported by the monomodal, skew-symmetric form characteristic of a single population governed by a log-hyperbolic distribution (shown superposed on the histogram) over the full range of fragment sizes. The scatter plot of $\log P$ against $\log A$ shown in Figure 6b yielded a least-squares line of regression [$R^2 = 94.8\%$] with $D_g = 0.99 \pm 0.07$, where the statistical measure $R^2 \equiv 1 - \dfrac{\text{mean square error of model}}{\text{variance of data}}$ quantifies the amount of variance in the data accounted for by a model (in this case, assumption of linearity in the double-log plot).

To ascertain that the sample size was adequate to represent the total population, we constructed a sequence of plots analogous to Figure 6b with each plot in the sequence based on a larger sample size than the preceding plot. This showed that there was little marginal utility to increasing the sample size beyond 151 since additional points had insignificant effect on the slope of the regression line. We also performed a statistical runs up/down test [26] on the chronological record of 151 fragment sizes to test for size bias in selection; the observed number of up/down runs was within 1 standard deviation of the theoretically expected mean number of such runs. This test is sensitive to violations of permutation invariance and has been used by two of the authors to test for nonrandom effects in alpha and beta decay of radioactive nuclei [27].

The unweighted mean of the three independent measurements is $\bar{D}_{\mathrm{RD}} = 1.06 \pm 0.09$. For comparison, Table 1 shows a representative sample (from Turcotte [28]) of values of D for other materials and fragmentation processes. No uncertainties on D were included in the reference from which the values in Table 1 were taken.

Although no physical sample of fragments follows a power law exactly, D nevertheless can provide a useful measure of the degree of irregularity of the particles created by a fragmentation process. The higher the value of D, the more space filling the irregular shape. For objects that are statistically invariant over a range of scale transformations, the degree of irregularity can be characterized by this one measure. As Table 1 shows, fractal dimensions of passive brittle materials generally fall between 2 and 3. According to Eq. (5), D cannot exceed 3, and reasons to doubt the accuracy of the last two entries in the table have been published [18]. Most noteworthy is the proximity of D values to 2.50 for processes of markedly different origin, ranging from the continuous and moderate (grinding; crushing) to the sudden and violent (chemical and nuclear explosions). Turcotte has hypothesized that fractal dimension should

increase with an increase in available energy density because fragmentation conserves mass and therefore volume, but not area—and the creation of area requires energy [16]. The numbers in the table do not appear to support this hypothesis, since one might have expected the fractal dimensions of fragments from chemical and nuclear explosions to be well above those of sands, clays, and glacial till produced by less energetic processes of comminution—although without error limits one cannot be sure of order statistics based on the table [29]. In any event, with any reasonable assignment of statistical uncertainties to the entries of the table it is clear that the consistent numerical values of the fractal dimension of Rupert's drops, obtained independently by three different methods, are by far lowest.

Table 1: Fractal Dimensions of Various Materials and Processes

MATERIAL	FRACTAL DIMENSION D
Rupert's drops (lead-crystal glass)	
Mass distribution D_M	1.17 ± 0.12
Particle distribution D_N	1.01 ± 0.08
Perimeter vs Area D_g	0.99 ± 0.07
Crushed quartz	1.89
Disaggregated gneiss	2.13
Disaggregated granite	2.22
FLAT TOP (chemical explosion 0.2 kt)	2.42
Asteroids (theory)	2.48
PILEDRIVER (nuclear explosion 61 kt)	2.50
Broken coal	2.50
Interstellar grains	2.50
Projectile fragmentation of basalt	2.56
Sandy clays	2.61
Terrace sands and gravel	2.82
Glacial till	2.88
Stony meteorites	3.00
Ash and pumice	3.54

The fractal dimensions we obtained for Rupert's drops fragments agree closely with the fractal dimensions reported by Suzuki *et al.* [30] for crushed glass by a measurement procedure comparable to our third method. Segregating the crushed glass sample by size into classes ranging from 15 μm to 950 μm, Suzuki *et al.* determined the fractal dimension of each class separately by applying Mandelbrot's "compass method" [31] (a variant of box counting) to the perimeter of two-dimensional projections of particle profiles. The reported fractal dimensions ranged from 1.0278 to 1.0440. No statistical errors were given, nor did the authors identify the type of glass used, or the state of the glass prior to crushing, or the manner by which the glass was crushed. The authors did not report particle or mass distributions of the glass fragments.

Other authors have obtained different values of D for the fractal dimension of crushed glass. Gilvarry and Bergstrom [32], investigating the fracture of solid glass spheres of diameter ~2.4 cm confined to a gelatin matrix and subjected to external compressive stress through tungsten carbide platens, reported double-log plots of cumulative mass versus size with unit slope. Corresponding to our Eq. (5c) for topological dimension $d = 3$, this result is equivalent to a fractal dimension $D = 2$. Odershedde *et al.* [6] obtained a scaling exponent equivalent to $D = 2$

for fragmentation of spherical balls of gypsum (calcium sulphate dihydrate) and found that the scaling depended on the shape of an object rather than on its material. However, in comparing fractal dimensions obtained from different experiments, it is critical to take note not only of object shape, but also of the scaling region. For example, Arakcheev and Lotov [33] cite an experiment yielding a scaling exponent equivalent to $D = 2.5$ for crushed glass, but the authors of the actual cited source [34], which reported $D = 2.35 \pm 0.11$, determined the fractal dimension of the *surface* of crushed glass as measured by a *molecular* "yardstick" in the approximate range of $4.6 \times 10^{-4} - 1.2 \times 10^{-2}$ microns.

If it should actually be the case that crushed glass and exploded metastable glass yield three-dimensional fragments of the same fractal dimension $D \sim 1$ over the tens to thousands of micron range, then our present work would show that fractal dimension is not a sensitive indicator of the internal dynamical state of glass. Nevertheless, an abnormally low (compared with brittle materials in Table 1) value of the fractal dimension of glass would still indicate that either (a) glass responds differently than most brittle materials do when subjected to fragmenting stresses of either internal or external origin, or (b) numerical values of the fractal dimension of glass depends on the specific measurement procedure, as can occur when fragments constitute a set of self-affine, rather than self-similar, objects.

4. Internal Energy and Explosion Dynamics

Regarding the internal energy of Rupert's drops, previous measurements have shown tensile stresses (near the axis) of about 100-160 MPa and compressive stresses (near the surface) of about 50-80 MPa [35]. If the shape of the drop head is taken roughly as a cylinder of diameter 2*R*, then the thickness δR of the compressive layer has been found to be $\sim \delta R / 2R \approx 0.13$ [14]. We can then estimate the internal strain energy per volume of the drop to be approximately [36]

$$U/V \simeq \left(3\sigma_t^2 \upsilon_t + 3\sigma_c^2 \upsilon_c\right) \Big/ Y \approx 0.24 \text{ MJ/m}^3 \qquad (9)$$

where $\sigma_t \approx 130$ MPa is the mean tensile stress, $\sigma_c \approx \frac{1}{2}\sigma_t \approx 65$ MPa is the mean compressive stress, $\upsilon_t = \left(1 - \delta R/R\right)^2 \approx 0.55$ and $\upsilon_c = 1 - \upsilon_t \approx 0.45$ are respectively the fractional volumes under tensile and compressive stresses, and $Y \approx 70$ GPa is Young's modulus. Putting this into perspective: To produce an equivalent strain energy density by application of an *external* force on initially unstressed glass would require a pressure $P_{\text{ext}} = \sqrt{Y\left(U/V\right)} \sim 130$ MPa or ~1,283 atm.

We have analyzed a high-speed video recording made at Corning research labs by Dr Steven E. DeMartino of the explosion of a single Rupert's drop with a frame speed reported to be 0.94 miles/s [1,513 m/s]. The video showed the propagation of the shock front from tail to head across a calibrated surface. In the sequence of frames that we selected from the recording to make the composite Figure 7, which progresses chronologically from left to right and top to bottom, one sees clearly the advance of the shock front behind which the fractured glass is opaque due to multiple light scattering. From the frame rate, size of photographed portion of drop (1 inch ~ 2.5 cm), and calibration spacing ($1/8$ inch ~ 0.3125 cm), we estimated a shock speed of about 1,130-1,140 m/s. For comparison, the speed of sound in lead-crystal glass is in the range of 3,800-4,000 m/s. As shown in the Figure, fragments of glass began to disperse outward from the surface only after the shock wave propagated entirely through the drop. As expected, therefore, the shock front propagated with greater velocity through the tensile core than through the compressed surface layer.

The full video continued well beyond the last frame shown in Figure 7. By counting the number of frames between the time the shock wave reached the tip of the head and the time when the surface of scattered fragments moved outward a distance equal to the calibration length we estimated the velocity of the dispersing particles to be about 15-25 m/s. If it is assumed that the

strain energy released in the core goes primarily into the kinetic energy of the particles of the compressed surface layer, then a rough measure of the kinetic energy density is given by

$$K/V = \frac{1}{2}\rho\left\langle v^2\right\rangle \upsilon_c \approx 0.22 \text{ MJ/m}^3 \tag{10}$$

where $\rho = 2{,}400$ kg/m^3 is the mass per volume of glass, and the second moment $\left\langle v^2\right\rangle$ of the speed was calculated by assuming a normal velocity distribution of mean 20 m/s and variance 10^2 m^2 / s^2 as estimated from the Corning video. The kinetic energy density in Eq. (10) is consistent with the internal strain energy density estimated in Eq. (9).

5. Discussion and Conclusions

The disintegration of a Rupert's drop may be understood in broad outline on the basis of the pioneering theoretical work of A. A. Griffith, according to which the fracture of a brittle material like glass arises from growth of pre-existing microcracks [37]. The energy required for creating new areas of free surface as the crack grows is acquired from the internal elastic energy of the surrounding medium. However, this growth occurs only if (a) the stress field around the microcrack is tensile and (b) the product of the stress and the square root of the crack diameter exceeds a material-dependent critical parameter. Microcracks in the outer surface of a Rupert's drop cannot grow, even when the head of the drop is subject to significant impact or pressure, because the medium within which these cracks are embedded is in a state of high compressive stress. However, fracture of the thin cylindrical tail by application of an external force penetrates the core, which is in a state of tensile stress, thereby initiating a shock front that propagates in both directions with a speed comparable to that of sound waves in glass as demonstrated in the previous section.

Although Griffith's theory and more recent extensions to fractal cracks in solids [38,39] sheds light on the explosive metastability of Rupert's drops, specific details of the fragmentation mechanism are still uncertain. One would like to know, for example, how cracks propagate three-dimensionally through the drop just prior to the actual explosion, whether crack propagation is fractal or not, whether the fragmentation is in some sense universal or largely sensitive to the properties of the specific medium and its inhomogeneities.

In our statistical study of lead-crystal glass fragments from exploded Rupert's drops, we determined the mass density function $m(s)$, mass distribution $M(s)$, particle density function $n(s)$, and particle distribution $N(s)$ as functions of particle size s. These experimental distributions can be tested against theoretical fragmentation models that predict the form of the particle or mass densities or the fractal dimension of the set of fragments. By and large, the many theories of fragmentation developed over the years fall into two broad categories: (a) analytical deterministic or statistical theories based on general physical or mathematical principles, and (b) stochastic theories that simulate fragmentation by means of specific computationally tractable models executed numerically on a discrete lattice. This partitioning is meant to be heuristic, not definitive, since some theories have elements of both classes. The first category would include, for example, Griffith's theory derived from the general theory of elasticity, or statistical theories based on the principle of maximum entropy [40]. The second category would include various mechanical models of fracture propagation, such as the diffusion-limited aggregation model [DLA] [41] or random-fuse model [42]. Given the huge number of fragmentation models, we can consider in this concluding section only such studies as may bear directly on the experimental results we obtained.

Among the earliest papers in the analytical category, Kolmogorov [43] deduced that for particles created by repetitive fracture (e.g. grinding) $n(s)$ should be of log-normal form reducing to $n(s) \propto s^{-1}$ when the width parameter is sufficiently large. From Eq. (5), this would

imply $D_n = 0$. Gilvarry's theory of single fracture by an external stress system [44], predicated on flaw activation by stress waves, led to the asymptotic form equivalent to $M(s) \propto s^{-1}$, implying $D_M = 2$, which was observed experimentally by Gilvarry and Bergstrom [32] for crushed glass spheres. Both predictions, however, appear to be in conflict with our experimental findings. The distributions we obtained were not of log-normal form, and the fractal dimension of Rupert's drops fragments was found to be $D_{\mathrm{RD}} \approx 1$. Moreover, high-speed photographic studies of Rupert's drops showed an absence of stress waves in shadowgraphs of drops exploded in water [14].

Applying the principle of maximum entropy to fragmentation by a fast, sudden process, Englman [45] derived, on the basis of an assumed energy function $e(s)$ per particle, a 2-parameter mass density of the form $m(s)_{\mathrm{ME}} = C\left[2\nu(s/\hat{s})^{-1} + 1 + \nu(s/\hat{s})^{2}\right]^{-1}$, where C is an empirical constant, $\hat{s}$ is a scaling parameter, and $\nu < 1$ is a shape parameter. Although the function displays a sharp rise and long fall-off with s, such as in Figure 3a, a graphical survey of the theoretical shapes taken by $m(s)_{\mathrm{ME}}$ for wide range of positive values of $\hat{s}$ and ν failed to reproduce our distribution $m(s)$ for Rupert's drop fragments. In particular, the predicted distribution rose with incorrect curvature and fell off too slowly. Since all the physics resides in the function $e(s)$, our experimental distributions may help guide construction of a more appropriate energy function. We found empirically that a modified mass density $\tilde{m}(s) = C\left[2\nu(\hat{s}/s)^{-a} + 1 + \nu(s/\hat{s})^{2a}\right]^{-1}$ with $a > 1$ matched the experimental profile of Figure 3a considerably better. It remains to be seen, however, whether such a modified form may have a theoretical basis.

In the category of lattice models, fragmentation studies by crack branching have been published—see, for example [46, 47]—based on the assumption that at each level r of a hierarchy of subdivided geometric elements (e.g. cubes) a fragment will further split into f_r fragments with a probability p_r. In the simplest case, developed for isotropic brittle solids, p and f are independent of r, and the model is scale invariant leading to the fractal dimension $D = d\ln(pf)/\ln f$ where d is the topological dimension. The models do not furnish *a priori* values for p and f and therefore do not predict the fractal dimension D. Because such models were created in the first place to produce fractal branching, they lead to power-law distributions which can be only asymptotic approximations to the actual empirical distributions reported here. Nevertheless, if one applies the fractal cube model to our results for fragmentation of Rupert's drops, assuming the previously proposed mechanism of crack bifurcation in a space of d dimensions for which $f = 2^d$ and $p = 2^{D-d}$ with $D = 1$ and $d = 3$, one obtains $p = 0.25$. Whether or not Rupert's drops actually fracture by crack bifurcation, however, remains to be established. Experimentally, we did not see signs of crack bifurcation in magnified images of the high-speed video of a single exploding drop. To see such detail would in any event have been difficult because fracturing rendered the affected regions practically opaque.

Of particular potential interest are computer simulations of the rupture process whereby the Lamé equation or Cosserat equation for a linear elastic medium of specified properties is discretized and solved for the displacement field by an iterative procedure [48]. Within each cycle of iteration, the deterministic set of resulting coupled equations is supplemented by a constitutive relation applied to each bond of the lattice model that determines the breaking threshold value of strain δ and a probability function p, dependent on strain usually in the form $p \propto \delta^{\eta}$ for some adjustable parameter η, which determines stochastically which bonds will break. A characteristic

feature of this model is that it led to fractal fracture patterns in the absence of noise or long-range time correlations. Choices of η and the criteria for rupture corresponding to crack propagation in a medium under uniaxial tension were shown to produce fractal dimensions of about 1.10-1.25 [48,49], which is close to our experimental result for Rupert's drops. Such a process is analogous to stress corrosion cracking in metals, which can progress very rapidly, leading to catastrophic failure. It is possible that this fracture model captures essential features of the tensile stress distribution and shock-induced disintegration in Rupert's drops. However, it should be noted that the above fractal dimensions produced by the model pertain to single crack patterns and not necessarily to particle fragments. Of particular interest is the geometric form of the computer-generated crack patterns, which are more complex than simple bifurcation patterns and might help account for the distribution of Rupert's drops fragments if the model were extended to three dimensions.

Mandelbrot has noted that different definitions of fractal dimension of a set of objects should yield the same numerical value if the objects are self-similar [31]. In the fragmentation of Rupert's drops, we have consistently obtained the same numerical value of D within statistical uncertainties by three procedures, two of which were based on the statistical definition $N(s) \sim s^{-D}$ and one of which was based on the geometric definition $P \sim A^{D/2}$. Nevertheless, it is possible that the fragments of internally exploded glass do not constitute a set of self-similar objects since tensile and compressive stresses within the glass may be distributed inhomogeneously, and particles originating in the core may be distributed differently from particles coming from the surface layers. In the next phase of our research we plan to examine this hypothesis by investigating individual glass drops exploded within a confining matrix so as to permit statistical analysis of fragments drawn separately from areas of tension and compression. Interestingly, such an observation (although not statistical analysis) is alleged to have been made by Robert Hooke who drew the interior of a Rupert's drop in his classic work *Micrographia* [50]. The conically shaped fragments, however, bear no resemblance to actual fragments, and it is more likely that Hooke imagined, rather than observed, the interior of a Rupert's drop.

Acknowledgment: M. P. Silverman gratefully acknowledges samples of Rupert's drops fragments and the video recording provided by Dr. Steven DeMartino, Manager of Reliability, Optical, Electrical and Mechanical Sciences, Corning Glass Corporation.

PHYSICA SCRIPTA
doi:10.1088/0031-8949/85/06/065403

REFERENCES

[1] G. B. Clark, *Principles of Rock Fragmentation* (Wiley, New York, 1987).
[2] M. A. Lange and T. J. Ahrens, "Fragmentation of ice by low velocity impact", *Proc. Lunar Planet. Sci.* **12B** (1981) 1667-1687.
[3] J. S. Mathis, W Rumpl, and K H Nordsieck, "The Size Distribution of Interstellar Grains", *ApJ* **217** (1977) 425-433.
[4] W. K. Brown and R. R. Karpp, "Fragmentation of the Universe", *Astrophysics & Space Science* **94** (1983) 401-412.
[5] X. Camp and J. Hufner, Nuclear spallation-fragmentation reactions induced by high-energy projectiles", *Phys. Rev. C***24** (1981) 2199-2209.
[6] L. Oddershede, P. Dimon, and J. Bohr, "Self-Organized Criticality in Fragmenting", *Phys. Rev. Lett.* **71** (1993) 3107-3110.
[7] E. S. C. Ching, S. L. Lui, and K-Q Xia, "Energy dependence of impact fragmentation of long glass rods", *Physica* A **287** (2000) 83-90.
[8] S Oka, *Fluidized Bed Combustion* (Marcel Dekker, 2003, New York) 232-236.
[9] B. Bozic, "Control of Fragmentation by Blasting", *Rud.-geol.-naft. zb.* **10** (1998) 49-57; available at http://www.scribd.com/doc/73720355/Control-of-Fragmentation-by-Blasting.
[10] J. A. Astrom, B. L. Holian, and J. Timonen, "Universality in Fragmentation", *Phys. Rev. Lett.* **84** (2000) 3061-3064.
[11] E. Bouchaud, G. Lapasset, and J. Planès, "Fractal Dimension of Fractured Surfaces: a Universal Value?", *Europhys. Lett.* **13** (1990) 73-79.
[12] L. Brodsley, C. Frank, and J.W. Steeds, "Prince Rupert's Drops", *Notes Rec. R. Soc. Lond.* **41** (1986) 1-26.
[13] It is reported that King Charles II of England would offer a glass drop to a courtier in such a way as to break the tail as he relinquished the drop, thereby causing the drop to explode in the courtier's hand as a joke. [Corning Museum of Glass: http://www.cmog.org/dynamic.aspx?id=5660#.TwOFi0Zb17s.]
[14] S. Chandrasekar and M. M. Chaudhri, "The explosive disintegration of Prince Rupert's drops", *Phil. Mag.* B **70** (1994) 1195-1218.
[15] M. M. Chaudhri, "Crack bifurcation in disintegrating Prince Rupert's drops", *Phil. Mag. Lett.* **78** (1998) 153-158.
[16] D. L. Turcotte, "Fractals in Geology and Geophysics", *PAGEOPH* **131** (1989) 171-196.
[17] B. B. Mandelbrot, *The Fractal Geometry of Nature* (Freeman, New York, 1983).
[18] S. W. Tyler and S. W. Wheatcraft, "Fractal Scaling of Soil Particle-Size Distributions: Analysis and Limitations", *Soil Sci. Soc. Am. J.* **56** (1992) 362-369.
[19] E. Perfect, V. Rasiah, and B. D. Kay, "Fractal Dimensions of Soil Aggregate-Size Distributions Calculated by Number and Mass", *Soil Sci. Soc. Am. J.* **56** (1992) 1407-1409.
[20] E. Perfect, "Fractal models for the fragmentation of rocks and soils: a review", *Engineering Geology* **48** (1997) 185-198.
[21] Mandelbrot, *op. cit.* p. 110.
[22] O. Barndorff-Nielsen, (a) "Exponentially Decreasing Distributions for the Logarithm of Particle Size", *Proc. Roy. Soc. Lond. A* **353** (1977) 401-419, (b) "Hyperbolic Distributions and Distributions on Hyperbolae", *Scandinavian Journal of Statistics*, **5** (1978) 151-157.
[23] N. R. J. Fieller, E. C. Fienley, and W. Olbricht, "Statistics of Particle Size Data", *Applied Statistics* **41** (1992) 127-146.
[24] C. Moreno and H. Bruzzone, "Parameters' variances of a least-squares determined straight line with errors in both coordinates", *Meas. Sci. Tech.* **9** (1998) 2007-2011.
[25] M. P. Silverman, W. Strange, and T. C. Lipscombe, "Quantum test of the distributions of composite physical measurements", *Europhys. Lett.* **67** (2004) 572-578.

[26] H. Levene and J. Wolfowitz, "The Covariance Matrix of Runs Up and Down", *Ann. Math. Stat.* **15** (1944) 58-69.
[27] M. P. Silverman, W. Strange, C. Silverman, T. C. Lipscombe, "Tests for randomness of spontaneous quantum decay", *Phys. Rev.* A **61** 042106 (1-10)
[28] Turcotte, *op. cit.* p. 174.
[29] M. P. Silverman and W. Strange, "The distribution of composite measurements: How to be certain of the uncertainties in what we measure", *Am. J. Phys.* **72** (2004) 1068-1081.
[30] M. Suzuki, Y. Muguruma, M. Hirota, and T. Oshima, "Fractal dimensions of particle projected shapes", *Advanced Powder Technol.* **1** (1990) 115-123.
[31] B. B. Mandelbrot, "Self-Affine Fractals and Fractal Dimension", *Phys. Script.* **32** (1985) 257-260.
[32] J. J. Gilvarry and B. H. Bergstrom, "Fracture of Brittle Solids. II. Distribution Function for Fragment Size in Single Fracture (Experimental), *J. Appl Phys*. **32** (1961) 400-410.
[33] A. S. Arakcheev and K. V. Lotov, "Model of brittle destruction based on hypothesis of scale similarity", paper P1.063 presented at 38th EPS Conference on Plasma Physics (2011); http://ocs.ciemat.es/EPS2011PAP/pdf/P1.063.pdf.
[34] D. Avnir, D. Farin, and P. Pfeifer, "Molecular Fractal Surfaces", *Nature* **308** (1984) 261-263.
[35] W. Johnson and S. Chandrasekhar, "Rupert's glass drops: Residual-stress measurements and calculations and hypotheses for explaining disintegrating fracture", *J. Mat. Proc. Tech*. **31** (1992) 413-440.
[36] J. M. Barsom, "Fracture of Tempered Glass", *Journal of the American Ceramic Society* **51** (1968) 75-78.
[37] A. A. Griffith, "The Phenomena of Rupture and Flow in Solids", *Phil. Trans. Roy. Soc. Lond.* A **221** (1921) 163-198.
[38] G. P. Cherepanov, A. S. Balankin, and V. S. Ivanova, "Fractal Fracture Mechanics—A Review", *Engineering Fracture Mechanics* **51** (1995) 997-1033.
[39]A. Carpinteri, "Scaling Laws and Renormalization Groups for Strength and Toughness of Disordered materials", *Int. J. Solids Structures* **31** (1994) 291-302.
[40] E. T. Jaynes, "Information Theory and Statistical Mechanics" Part I, *Phys. Rev.* **106** (1957) 620-630; Part II **108** (1957) 171-190.
[41] P. Meakin, G. Li, L. M. Sander, E. Louis, and F. Guinea, "A simple two-dimensional model for crack propagation", *J. Phys. Math. Gen.* **22** (1989) 1393-1403.
[42] P. M. Duxbury, P. L. Leath, and P. D. Beale, "Breakdown properties of quenched random systems: The random-fuse network", *Phys. Rev.* B **36** (1987) 367-380.
[43] A. N. Kolmogorov, "On the Logarithmic Normal Distribution of Particle Sizes under Grinding", *Dokl. Akad. Nauk. SSSR* **31** (1941), 99-101, republished in A. N. Shiryayev, Ed., *Selected Works of A. N. Kolmogorov* (Kluwer, Boston, 1992) 281-284.
[44] J. J. Gilvarry, "Fracture of Brittle Solids. I. Distribution Function for Fragment Size in Single Fracture (Theoretical)", *J. Appl. Phys*. **32** (1961) 391-399.
[45] R. Englman, "Fragments of matter from a maximum entropy viewpoint", *J. Phys.: Condens. Matter* **3** (1991) 1019-1053.
[46] A. C. Palmer and T. J. O. Sanderson, "Fractal Crushing of Ice and Brittle Solids", *Proc. Roy. Soc. Lond. A* **433** (1991) 469-477.
[47] J. Astrom and J. Timonen, "Fragmentation by Crack Branching", *Phys. Rev. Lett.* **78** (1997) 3677-3680.
[48] H. J. Herrmann, "Patterns and Scaling in Fracture", *Phys. Script.* T**38** (1991) 13-21.
[49] H. J. Herrmann, "Fractal Shapes of Determnistic Cracks", *Europhys. Lett.* **10** (1989) 147-152.
[50] Robert Hooke, *Micrographia* (Dover, New York, 1961) Fig Y (between pages 10 and 11), pp 42-43. This is a facsimile reproduction of the first edition published by the Royal Society in 1665.

PHYSICA SCRIPTA
doi:10.1088/0031-8949/85/06/065403

FIGURES

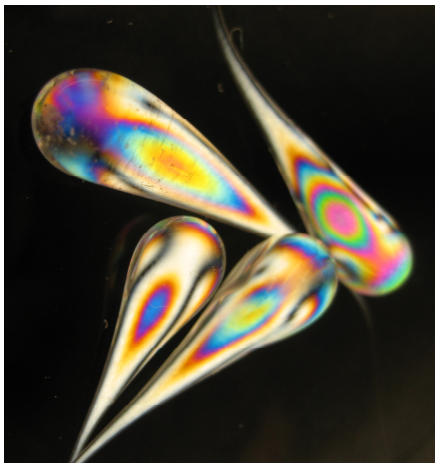

Figure 1: Soda-lime Rupert's drops between crossed polarizers.

Figure 2: Unexploded Rupert's drop (left) and powder (right) resulting from the explosion following cracking of the tail. (Courtesy of Corning Museum of Glass.)

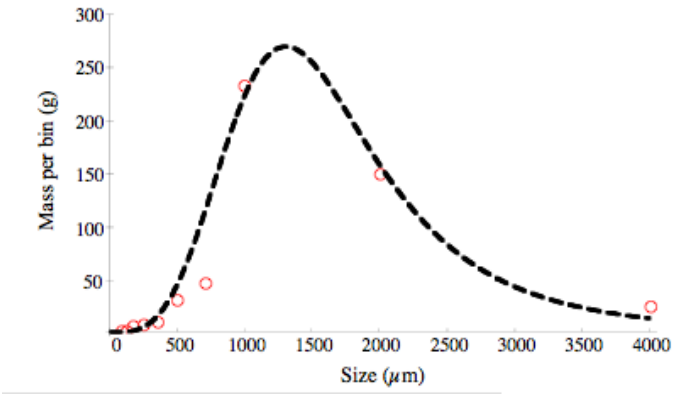

Figure 3a: Plot of mass per bin (in g) against mean mesh size (in μm) of the sieved sample (red circles) of lead-crystal Rupert's drops fragments. Theoretical density $m(s)$ of Eq. (7) is superposed (dashed curve). [Parameters: $A = 8.85$, $a = 3.30$, $b = -0.55$, $\mu = 7.30$, $\delta = 0.74$.]

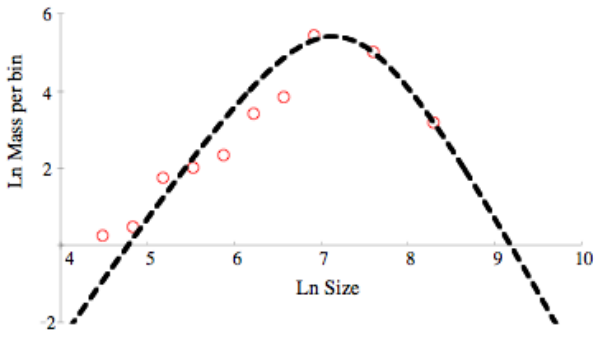

Figure 3b: Double-ln plot of mass per bin against mean size (red circles). Log hyperbolic density is superposed (dashed line). [Parameters: $A = 8.98$, $a = 3.60$, $b = -0.40$, $\mu = 7.25$, $\delta = 0.95$.]

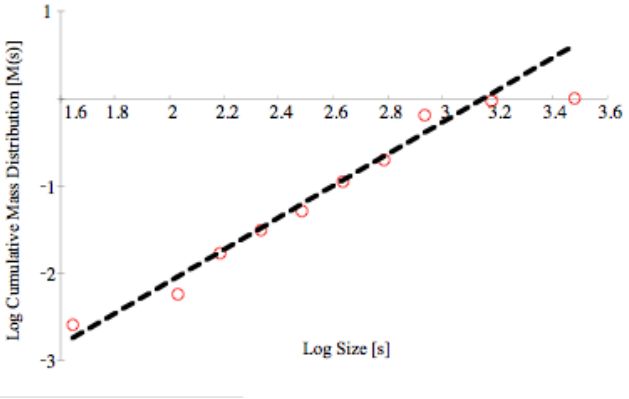

Figure 4: Double-log plot of cumulative mass $M(s)$ against mean size s (red circles) for same sample as in Figure 3 with superposed least-squares line of regression (dashed line) excluding the fraction at $s_{\max}$. Same units as in Figure 3.

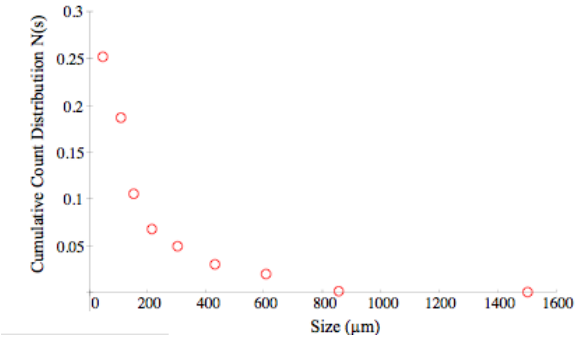

Figure 5a: Plot of cumulative particle number $N(s)$ against mean size s for the same sample as in Figure 3.

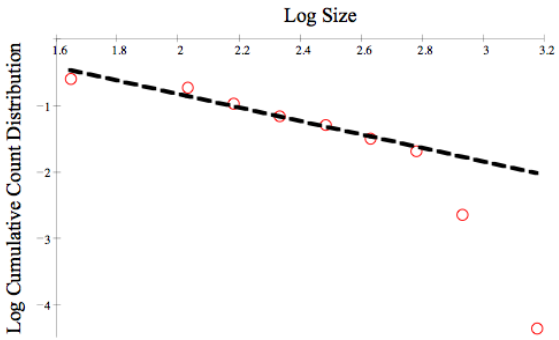

Figure 5b: Corresponding double-log plot of cumulative particle number against mean size (red circles) with superposed least-squares line of regression (dashed line) excluding two fractions of largest size.

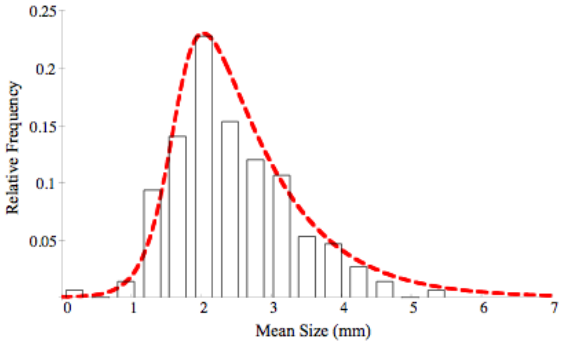

Figure 6a: Histogram of mean size of 151 fragments with superposition of log hyperbolic density (dashed line). [Parameters: $A = 0.60$, $a = 1.20$, $b = 0.72$, $\mu = 1.70$, $\delta = 0.43$.] Unit of length is mm.

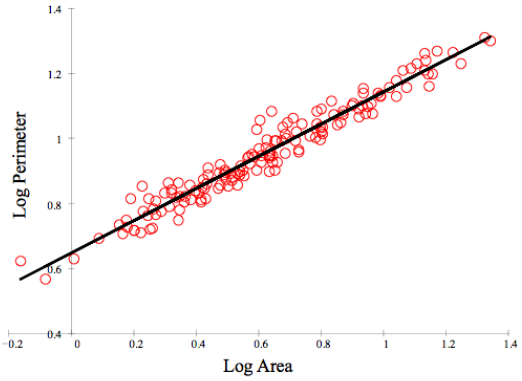

Figure 6b: Corresponding double-log scatter plot of observed perimeter against area (red circles) with least-squares line of regression superposed (solid line).

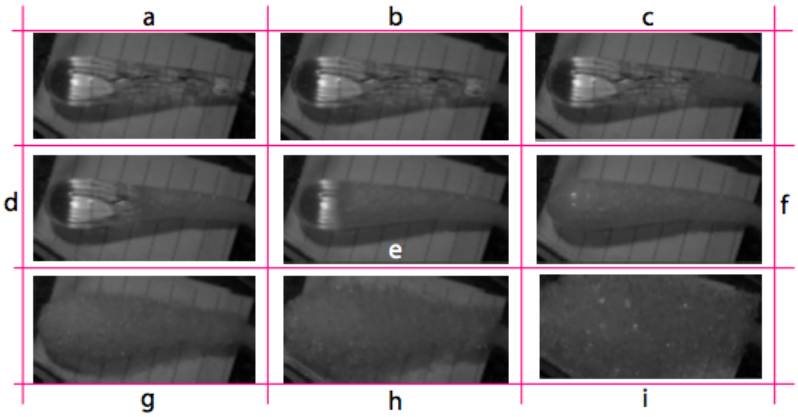

Figure 7: Chronological progression (a to i) of the propagation of the shock front through a Rupert's drop following rupture of tail. Dispersal of particles from the surface begins after total fracturing of the core (frame f). [Figure constructed from a video provided by Dr. Steven DeMartino of the Corning Glass Corporation.]